



# 1 Impact of hydro-meteorological conditions and flash drought 2 duration on post-flash drought recovery time patterns

3 Mengge Lu<sup>1,2</sup>, Huaiwei Sun<sup>1,3,4,5\*</sup>, Yong Yang<sup>1</sup>, Jie Xue<sup>3</sup>, Hongbo Ling<sup>3</sup>, Hong Zhang<sup>6</sup>, Wenxin  
4 Zhang<sup>2</sup>

5 <sup>1</sup>School of Civil and Hydraulic Engineering, Huazhong University of Science and Technology, Wuhan 430074, China.

6 <sup>2</sup>Department of Physical Geography and Ecosystem Science, Lund University, Sölvegatan 12, 22362 Lund, Sweden.

7 <sup>3</sup>State Key Laboratory of Desert and Oasis Ecology, Xinjiang Institute of Ecology and Geography, Chinese Academy of  
8 Sciences, Urumqi 830011, China.

9 <sup>4</sup>Hubei Key Laboratory of Digital River Basin Science and Technology, Huazhong University of Science and Technology,  
10 Wuhan 430074, China.

11 <sup>5</sup>Institute of Water Resources and Hydropower, Huazhong University of Science and Technology, Wuhan 430074, China.

12 <sup>6</sup>School of Engineering and Built Environment, Griffith University, Gold Coast Campus, 4222, QLD, Australia.

13

14 *Correspondence to:* Huaiwei Sun ([hsun@hust.edu.cn](mailto:hsun@hust.edu.cn))

15

16

17 **Abstract.** Recovery time, which refers to the duration an ecosystem needs to revert to its pre-drought state, is a fundamental  
18 aspect of ecological resilience. Recently, flash droughts (FDs) characterized by rapid onset and development have been  
19 gained recognition. Nevertheless, the spatiotemporal patterns of recovery time and the factors that affect it remain largely  
20 unknown. In this study, we set up a novel method to investigate the recovery time patterns of terrestrial ecosystem in China  
21 based on gross primary productivity (GPP) by employing the Random Forest (RF) regression model and the Shapley  
22 Additive Prediction (SHAP) method. A random forest regression model was developed for analysing the factors influencing  
23 recovery time and establish response function functions through partial correlation for typical flash drought recovery periods.  
24 Additionally, the dominant driving factors of recovery time determined by using the SHAP method. Results reveal an  
25 average recovery time of approximately 37.5 days across China, with central and southern regions experiencing the longest  
26 recovery time. Post-flash drought radiation emerges as the primary environmental factor, followed by aridity index and post-  
27 flash drought temperature, particularly in semi-arid/sub-humid areas. Temperature exhibits a non-monotonic relationship  
28 with recovery time; with excessively cold or overheated temperatures leading to longer recovery times. Herbaceous  
29 vegetation recovers more rapidly than woody forests, with deciduous broadleaf forests demonstrating the shortest recovery  
30 time. This study provides valuable insights into comprehensive water resource and ecosystem management, and it will be  
31 helpful in large-scale drought monitoring.

32

33



## 34 **1 Introduction**

35 Climate change has exacerbated drought, which could have significant implications for the achievement of Sustainable  
36 Development Goals (SDGs) (Lindoso et al., 2018). Among the 17 SDGs proposed in the 2030 Agenda, at least 5 of them are  
37 directly associated with drought, including Goal 6 “Clean water and sanitation”, Goal 11 “Sustainable cities and  
38 communities”, Goal 12 “Responsible production and consumption”, Goal 13 “Climate action”, and Goal 15 “Life on land”  
39 (Zhang et al., 2019; Nilsson et al., 2016). Flash droughts, characterized by rapid onset and intensification, have recently  
40 gained recognition by hydrologist and general public worldwide (Yuan et al., 2023). These have a significant impact on the  
41 productivity, photosynthesis, and latent heat flux of the ecosystem (Zhang et al., 2020a; Yang et al., 2023). The impacts of  
42 flash droughts are not only reflected during the events but also have legacy effects post the events (Liu et al., 2023).  
43 Recovery time, defining the duration an ecosystem requires to recover its pre-drought state, is a fundamental aspect of  
44 ecological resilience (Schwalm et al., 2017; Wu et al., 2017). It is related to ecological states as it may trigger a critical  
45 "tipping point" in the ecosystem leading to a transition to a new state (Lenton et al., 2008). With the anticipation of more  
46 frequent and severe flash droughts in the future (Sreeparvathy & Srinivas, 2022), it is of paramount importance to explore  
47 post-flash drought recovery trajectories (Jiao et al., 2021).

48 Drought recovery characteristics have been widely observed at the ecosystem scale, usually determined through tree ring  
49 records, productivity or greenness observation, and satellite retrieval (Gazol et al., 2017; Kannenberg et al., 2019). These  
50 studies have found varied recovery times across different regions and ecosystems. For different ecosystem types, grasslands  
51 have a longer recovery time compared to other land covers due to their shallow-rooted plants and lower soil water retention  
52 capacity (Hao et al., 2023). In contrast, the recovery time in croplands is more susceptible to interference by human farming  
53 systems (Darnhofer et al., 2016). For forests, mixed forests can recover quickly, while deciduous broadleaf forests have the  
54 longest recovery time (He et al., 2018). When comparing hydro-meteorological conditions, semi-arid and semi-humid  
55 regions have a longer recovery time compared to humid and arid regions (Zhang et al., 2021).

56 However, the contribution of driving factors in flash drought recovery remains unclear in previous studies. For example,  
57 some results reveal that the background value, drought return interval, post-drought meteor-hydrological conditions, and  
58 drought attributes (duration, intensity, etc.) play an important role in regulating drought recovery (Kannenberg et al., 2020).  
59 This may be due to the fact that the lower the background value, the more severe the damage to the ecosystem, the more  
60 abnormal the meteor-hydrological conditions after drought, and the longer the required drought recovery time (Fu et al.,  
61 2017). Greater intensity and longer duration can lead to substantial drought losses (Godde et al., 2019). Additionally, more  
62 favorable post-drought meteor-hydrological conditions (e.g., increased precipitation and suitable temperature) increase the  
63 probability of complete recovery (Jiao et al., 2021). The physiological regulation of plants, including alterations in leaf water  
64 potential and phenology, also plays a crucial role in this process (Miyashita et al., 2005).



65 Although the impact of flash droughts on ecosystems and their subsequent damage has been extensively studied, the  
66 recovery process requires more attention for a better understanding of flash droughts. It has been reported that both SIF and  
67 SIF yield values showed a declining trend post-flash drought (Yao et al., 2022), while 95% of the GPP in the Indian region  
68 responded to flash droughts, with an average response time of 10-19 days (Poonia et al., 2021). However, these studies  
69 predominantly focus on the response of ecological indicators, particularly the decrease caused by flash droughts, with limited  
70 attention given to the recovery process (Otkin et al., 2019). Notably, a substantial contrast exists in the definition of recovery  
71 stages between flash droughts and traditional slow droughts (Wang et al., 2016). These results lead to the conclusion that  
72 recovery is a part of the former, while the recovery phase of the latter usually occurs at the end of the event (Qing et al.,  
73 2022). Furthermore, some studies have concluded that the determination of flash drought recovery relies on changes in soil  
74 moisture or peak evapotranspiration intensity, while for traditional slow drought, it is mainly based on ecological or  
75 hydrological indicators (Xu et al., 2023). If we take China as a typical area for studying flash droughts, there were frequent  
76 flash drought events in China from southwest to central China from 1980 to 2021 (Wang et al., 2022a). Moreover, there may  
77 be more severe and frequent flash droughts in the future (Christian et al., 2023). Wang et al. (2023) conducted a study on the  
78 recovery of flash droughts in the Xiang River Basin and Wei River Basin in China and revealed that the majority of flash  
79 drought events in both basins recover within 28 days. However, to the best of our knowledge, there is currently a lack of  
80 studies on the recovery of flash drought and the factors influencing its spatiotemporal patterns across China.

81 Drought can lead to water shortages, reducing access to clean drinking water. Therefore, effective drought management is  
82 crucial for achieving SDGs. By collecting newly available datasets as well as hydro-meteorological variables in China, this  
83 study assesses the extent of the impact of flash drought post-flash drought, documents the time taken for recovery post-flash  
84 drought, and analyzes the factors contributing to variations in ecosystem recovery. The objectives of this study are to: (1)  
85 investigate the spatial pattern of post-flash drought recovery; (2) identify the most critical determinants of recovery; and (3)  
86 analyze the impact of various factors on flash drought recovery times. In the following sections, Section 2 provides a brief  
87 description of data and methods, followed by Section 3, which presents the results presented by novel methods applied.  
88 Then, we provide a detailed discussion in Section 4. Section 5 gives the conclusions with some more information presented  
89 in supplementary materials.

## 90 **2 Data and methods**

### 91 **2.1 Data**

#### 92 **2.1.1 Soil moisture datasets**

93 Daily root-zone soil moisture (SM) data for the period of 2001-2018 are obtained from Global Land Evaporation Amsterdam  
94 Model (GLEAM) (<https://www.gleam.eu/>). GLEAM estimates root-zone soil moisture using a multi-layer water balance  
95 approach. The depth of the root zone varies based on the type of land cover. For tall vegetation (e.g. trees), the depth is



96 divided into three layers (0-10 cm, 10-100 cm, and 100-250 cm); For low vegetation (e.g. grass), there are two layers (0-10  
97 cm and 10-100 cm); Bare soil only has one layer (0-10 cm) (Martens et al., 2017; Miralles et al., 2011). It has been widely  
98 applied in the identification and impact assessment of flash drought events (Zha et al., 2023). We utilized the bilinear  
99 interpolation method to resample SM from a spatial resolution of 0.25° to 0.1°, aligning it with the accuracy of other  
100 datasets. This method is appropriate for continuous input values, easy to implement, and generally effective in converting  
101 coarse input data into spatially refined output (Chen et al., 2020).

### 102 2.1.2 Hydro-meteorological datasets of affecting variables of recovery time

103 We analyze the recovery time considering multiple influencing factors such as meteorological variables, drought-related  
104 variables, and land cover (He et al., 2018). Meteorological data from the China Meteorological Forcing Dataset (CMFD),  
105 accessible at <https://westdc.westgis.ac.cn/>, is utilized for the period spanning 2001 to 2018 (Yang et al., 2019). The near-  
106 surface air temperature, downward shortwave radiation, downward longwave radiation, precipitation rate and wind speed are  
107 used in this study. VPD is calculated based on temperature, and specific humidity using Eq. (1) - (3) (Peixoto & Oort, 1996)  
108 (Zotarelli et al., 2020).

$$109 \text{ SVP} = 0.618 \exp\left(\frac{17.27T}{T+273.73}\right) \quad (1)$$

$$110 \text{ AVP} \approx \frac{q_s \cdot p}{\varepsilon} \quad (2)$$

$$111 \text{ VPD} = \text{SVP} - \text{AVP} \quad (3)$$

112 where SVP and AVP is saturated vapor pressure and actual vapor pressure (kPa), respectively. And  $T$  is temperatures  
113 (°C),  $q_s$  is the specific humidity,  $p$  is the atmospheric pressure (kPa),  $\varepsilon = 6.22$  is the ratio of water vapor molecular weight to  
114 dry air weight.

115 Aridity index is calculated as the ratio of precipitation to potential evapotranspiration. Typically, the multi-year average of  
116 the aridity index serves as an indicator of water availability and drought timing within a particular region (Huang et al.,  
117 2016). Aridity index is obtained from <https://doi.org/10.6084/m9.figshare.7504448.v5> (Zomer et al., 2022). To analyze the  
118 distinct responses of different vegetation types, we employ the MODIS dataset from the International Geosphere-Biosphere  
119 Programme (IGBP) MCD12C1 (Friedl et al., 2002) (Fig. S1).

### 120 2.1.3 Gross primary productivity

121 Gross Primary Productivity (GPP) is a commonly employed indicator for monitoring photosynthesis dynamics post drought  
122 (Gazol et al., 2018). This study uses the GPP datasets from Global MODIS and FLUXNET-derived Product. It has a spatial  
123 resolution of 0.1° and a daily time resolution (Joiner et al., 2021). To match the flash drought event, daily soil moisture data  
124 were aggregated to pentad-mean (five-days) data. This study chooses the growing seasons (April to October) from 2001 to  
125 2018 as the study period.



## 126 2.2 Method

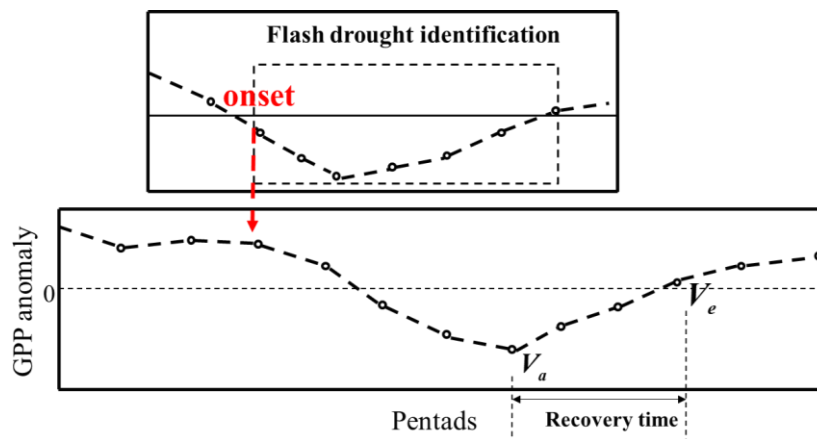
### 127 2.2.1 The identification of flash drought events and recovery time

128 In this study, we identify flash drought events by analyzing changes in soil moisture, taking into account their rapid  
 129 intensification and duration. Evaporation demand is often used as a warning indicator for flash droughts (Rigden et al.,  
 130 2020). Because it may overestimate flash droughts (Lesinger & Tian, 2022). To identify flash drought events, the daily soil  
 131 moisture data is aggregated into pentad-mean data. These averages are then converted into percentiles based on the  
 132 climatology of each pentad period during the growing season. According to the definition proposed by Yuan et al. (2019)  
 133 and Zhang et al. (2020a), we identify the flash drought event (Fig. 1 a&b). The speed of flash drought (Ospd) is the ratio of  
 134 the difference between the 40th percentile and the lowest percentile of the onset stage to the length of onset. The frequency  
 135 refers to the overall number of occurrences within a given time frame (e.g., per year or per decade). Severity is the  
 136 accumulated soil moisture percentile deficits from the threshold of 40%. On the basis of Wang et al. 2023 's definitions, we  
 137 defined the recovery time of vegetation production after a flash drought (Fig. 1):

$$138 \text{ GPP anomaly} = \frac{GPP - \mu_{GPP}}{\sigma_{GPP}} \quad (4)$$

139 where,  $\mu_{GPP}$  and  $\sigma_{GPP}$  are mean and standard deviation of the pentad time series of GPP.

140 When the GPP anomaly of post-flash drought is negative and reaches its minimum, it indicates the beginning of the recovery  
 141 stage. The recovery stage ends when the GPP anomaly returns to a positive value. However, if no flash drought event occurs  
 142 during the period of negative GPP anomaly or if the GPP anomaly is already negative before the onset of the flash drought  
 143 event, the GPP data series should be excluded.



144

145 **Figure 1. The identification of flash drought and recovery time.** (a) and (b) are flash drought identification base on SM  
 146 percentile. (b) Is detrended vegetation production index on a time series, 0 is defined as the threshold of a negative anomaly.  
 147 Below the dashed line represents that vegetation production is in a negative abnormal state. We quantify recovery time as:



148 the recovery time begins when the vegetation production loss reaches the maximum and ends when the detrended vegetation  
149 production index is above 0.

### 150 2.2.2 Response functions

151 Partial dependence plots based on the random forest algorithm are utilized for visualizing response functions (Schwalm et  
152 al., 2017; Sun et al., 2016). The analysis of partial dependence focuses on evaluating the marginal impact of a covariate (or  
153 independent variable) on the response variable, while keeping other covariates constant (Liaw & Wiener, 2002). It facilitates  
154 the exploration of insights within large datasets, particularly when random forests are primarily influenced by low-order  
155 interactions (Martin, 2014). In addition, it is valuable tools for identifying significant features, detecting non-linear  
156 relationships, and gaining insights into the overall behavior of a predictive model.

### 157 2.2.3 Attribution analysis of ecosystem recovery

158 In order to better understand the potential factors driving vegetation productivity recovery after flash droughts, we conduct  
159 attribution analysis. We selected downward radiation (the sum of downward shortwave radiation and downward shortwave  
160 radiation), temperature, wind speed, precipitation rate, VPD, flash drought speed (Ospd), flash drought severity (Osev), flash  
161 drought duration (Odur), aridity index, land cover types as explanatory variables. The feature importance of random forest  
162 can only indicate the extent to which the input variables influence the model's output, but it does not reveal how these input  
163 variables specifically impact the model's output (Wang et al., 2022b). The Shapley Additive Prediction (SHAP) method has  
164 emerged as a valuable tool that addresses the limitations of traditional machine learning methods  
165 (Štrumbelj&Kononenko,2014). As a result, the SHAP method is widely utilized in attribution analysis of variables (Wang et  
166 al., 2022b; Lundberg & Lee, 2017).

$$167 \varphi_m(v) = \sum_{S \in \mathcal{N} \setminus \{m\}} \frac{|S|!(|N| - |S| - 1)!}{|N|!} (v(S \cup \{m\}) - v(S)) \quad (5)$$

168 where,  $\varphi_m(v)$  represents the contribution of covariate  $m$ ,  $N$  denotes the set of all covariates,  $S$  is a subset of  $N$ , and  $v(S)$   
169 represents the value of that subset.

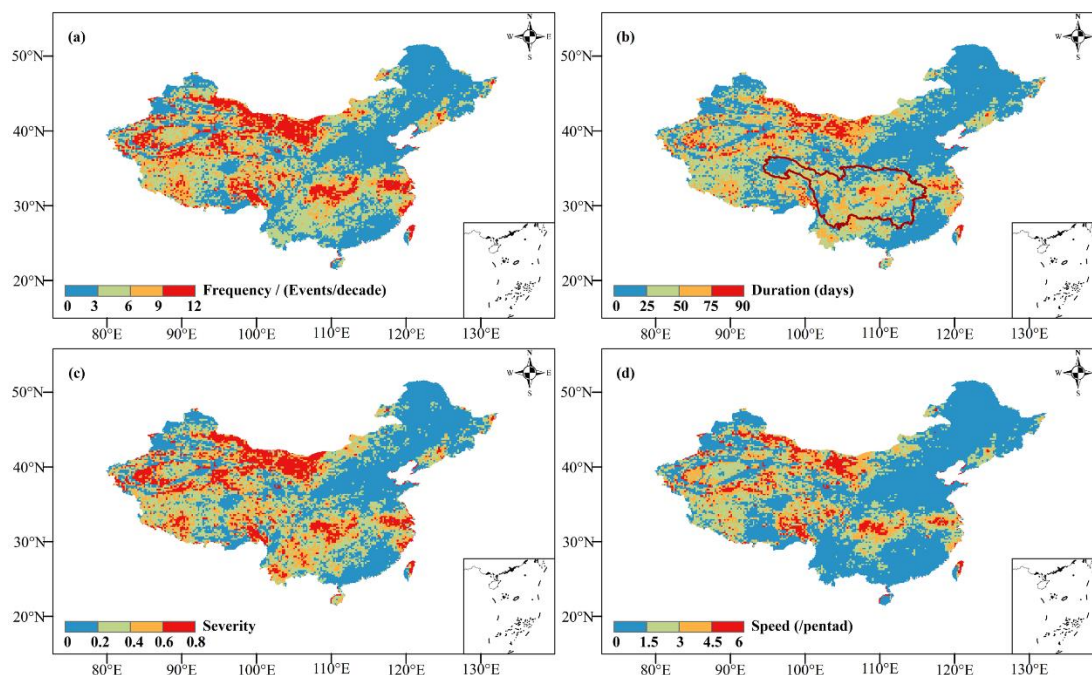
170 We utilized a random forest model and employed these variables as predictive factors to estimate the productivity recovery  
171 time for all study grid cells. Then, we used the SHAP value to quantify the marginal contribution of each predictive variable  
172 and rank their relative importance based on the average absolute SHAP value.



### 173 3 Results

#### 174 3.1 Characteristics of flash droughts

175 Figure 2 presents the frequency, duration, severity, and speed of flash droughts over China during 2001-2019.  
176 Approximately 7% of grids did not experience a flash drought event, while the remaining 93% of grids experienced at least  
177 one event. The middle and lower reaches of the Yangtze River exhibited a high frequency value with above 12  
178 events/decade, whereas other regions mainly ranged from 0 to 9 events/decade. There is a clear spatial pattern for the  
179 duration, ranging from 0 to 20 days over China. The Southwestern and the middle and lower reaches of the Yangtze River  
180 had longer durations, exceeding 90 days (Fig. S2). In addition to the higher severity of flash droughts in the southwest  
181 region, a similar spatial pattern was observed for severity and speed. Regarding speed, areas with faster speed were primarily  
182 concentrated in the lower reaches of the Yangtze River. Overall, the middle and lower reaches of the Yangtze River and the  
183 southwestern region are considered hot spots, although the latter's speed is not rapid.



184

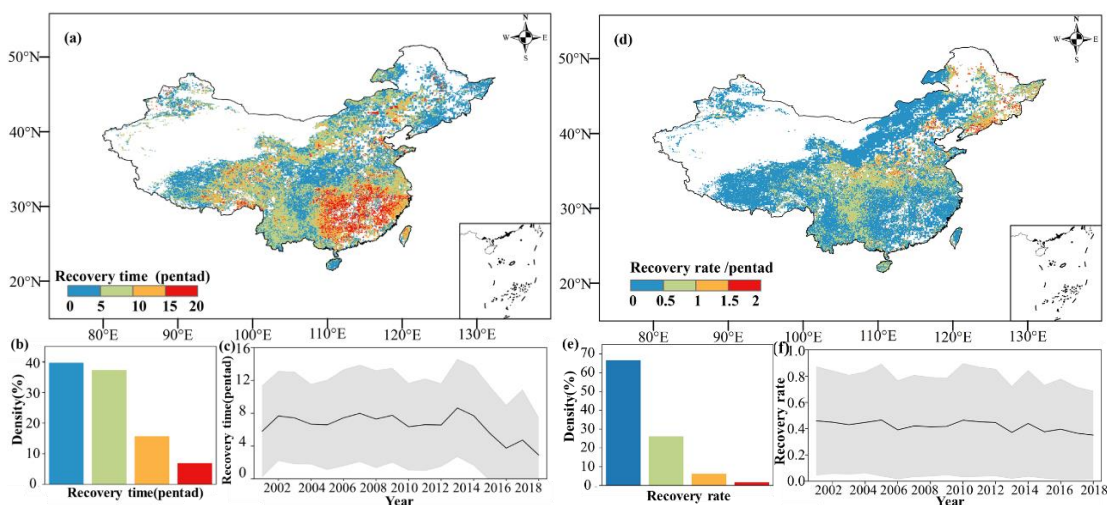
185 **Figure 2. Frequency (a), duration (b), severity (c), speed (d) of flash drought over China during 2001–2019.**

#### 186 3.2 Spatial pattern of ecosystem recovery time and recovery rate

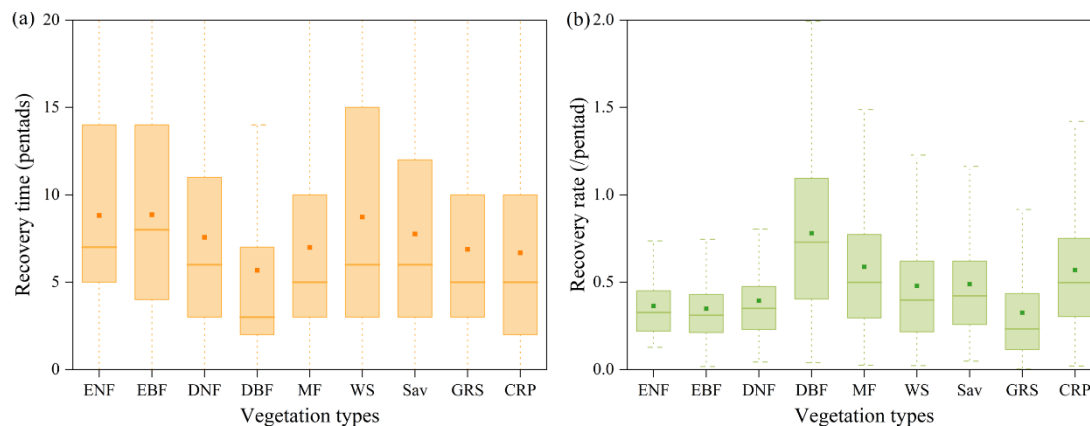
187 Vegetation productivity showed a clear response to flash droughts, and this response typically had a certain lag (Fig. S3).  
188 Ecosystems exhibited distinct spatial differences in recovery times to flash droughts (Fig. 3). The mean recovery time for  
189 Chinese ecosystems was 37.5 days (7.5 pentads) calculated by GPP. Most regions were able to recover to their normal state  
190 within 50 days. However, certain areas, such as central China and southern China, required 90 days or more to recover. In



191 terms of time series, there was no evident trend in the mean recovery time, with fluctuations occurring within 7.5 pentads.  
 192 On average, the recovery rate of grids in China ranged from 0 to 2 per pentad, and approximately 90% of grids had a  
 193 recovery rate of less than 1 per pentad. There is no significant trend in recovery rate over time. To further illustrate the  
 194 impact and recovery of flash droughts on different vegetation types, we calculated the recovery time and recovery rate for  
 195 each type (Fig. 4). Among the different vegetation types, DBF had a shorter recovery time and a higher recovery rate.  
 196 Additionally, CRP showed moderate recovery rates, while GRS had relatively low rates of recovery. This reflects the fact  
 197 that flash droughts had a more significant impact on GRS and resulted in greater productivity losses.



198  
 199 **Figure 3. Spatial pattern of recovery time (a-c) and recovery rate (d-f).** (a) and (d) represent the recovery time (pentad)  
 200 and recovery rate (/pentad) calculated by using GPP data respectively. (b) and (e) represent the density of different recovery  
 201 times and recovery rate respectively, the horizontal axis represents the recovery time (pentad), recovery rate (/pentad) and  
 202 the vertical axis is the density. Regions with sparse GPP or no droughts are masked with white.



203  
 204 **Figure 4. The recovery time and recovery rate across different vegetation types.** The vegetation types are: ENF  
 205 (evergreen coniferous forest), EBF (evergreen broad-leaved forest), DNF (deciduous coniferous forest), DBF (deciduous

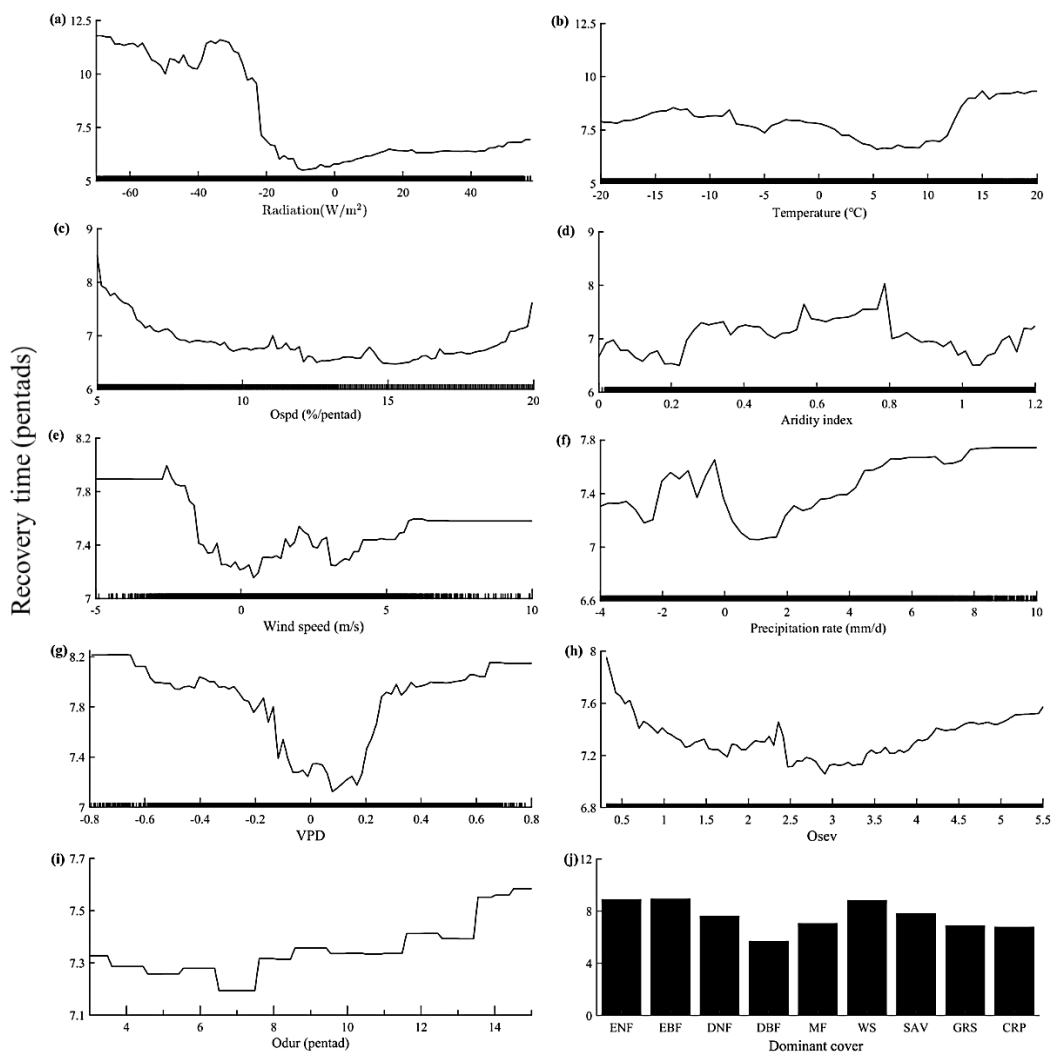




206 broad-leaved forest), MF (mixed forests), WS (closed shrubland, open shrubland, and woody savannas), SAV (savannas  
207 (temperate)), GRS (grasslands), CRP (croplands).

### 208 3.3 Response functions for flash drought recovery time

209 The random forest regression model explained 55% of the out-of-bag variance in recovery time (Fig. 5). Radiation emerged  
210 as the most influential factor impacting flash drought recovery time, with lower solar radiation conditions leading to  
211 prolonged the recovery time (Fig. 5a). Temperature did not exhibit a monotonic response in relation to recovery time.  
212 Excessively cold or overheated temperatures resulted in longer recovery times, whereas slightly higher temperatures  
213 promoted vegetation recovery (Fig. 5b). Specifically, a slight increase in temperature facilitated vegetation restoration, while  
214 higher temperatures extended the recovery time of flash droughts. This suggests that the projected rise in extreme high  
215 temperatures will further lengthen the recovery time (Li et al., 2019). In terms of flash drought characteristics, the difference  
216 in recovery time was related to the discrepancy in severity and duration, albeit to a lesser extent than speed (Fig. 5c, h & i).  
217 Recovery time increased in a stepwise manner as the duration increased. Ecosystems experiencing prolonged durations of  
218 flash droughts typically exhibit longer recovery times. In addition, semi-arid/sub-humid areas ( $0.2 < AI < 0.65$ ) have longer  
219 recovery times (Fig. 5d). The wind speed exhibited a bimodal pattern, indicating that the recovery time was shortest when it  
220 closely aligned with the multi-year average or was 3.5 times higher than the multi-year average (Fig. 5e). Adequate  
221 precipitation following a flash drought assisted in recovery, although excessively extreme precipitation could also hinder it  
222 (Fig. 5f). Extreme vapor pressure deficit (VPD), whether high or low, prolonged the recovery time (Fig. 5g). Among  
223 different vegetation types, herbaceous vegetation recovered more rapidly than woody forests. Deciduous broadleaf forests  
224 (DBF) demonstrated the shortest recovery time (Fig. 5j).



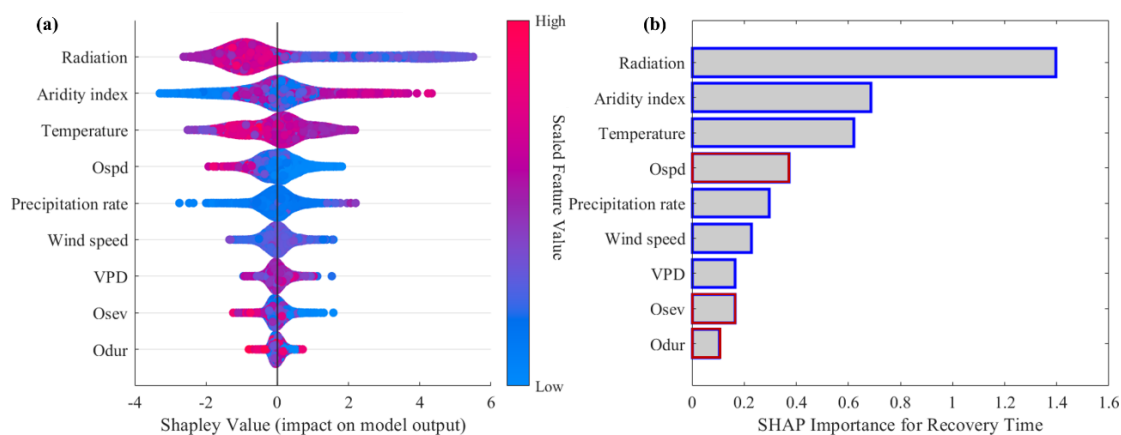
225  
 226 **Figure 5. Response functions for flash drought recovery time**, reflecting the response of recovery time to a single  
 227 dependent variable when others are unchanged. Note difference in the y-axis scales. The covariates a to j are the deviations  
 228 from the baseline. Positive (negative) indicates above (below) the average value.

### 229 3.4 Drivers of flash drought recovery time

230 We then performed an attribution analysis using SHAP method to quantify the relative importance of the considered  
 231 variables. The results were consistent with the results of section 3.3. In general, radiation and aridity index were the most  
 232 relevant controls of spatial variations of post-flash drought recovery time (Figure 6). Temperature was the third most  
 233 impactful variable overall, primarily due to its high impact in predicting the recovery time where it has an absolute mean  
 234 SHAP value of 0.62. Compared to other variables, the impact of speed and duration of flash droughts were relatively low. In  
 235 addition, during the process of flash drought recovery, the losses caused by flash droughts can also affect productivity



236 recovery. The relationship between recovery time and the attributes of flash drought (speed, severity, duration) is usually  
237 negative. That is to say, faster, more severe, and longer lasting flash droughts often have a longer recovery time.  
238 Specifically, the speed of flash droughts characteristics is one of the main controlling factors for recovery time.



239

240 **Figure 6. Identifying drivers of patterns of post-flash drought recovery time.** (a) The summary plot of SHAP values in  
241 random forest machine learning. (b) The SHAP Importance (averaged absolute SHAP values) for recovery time. Considered  
242 drivers include flash drought characteristics (in red), post-flash drought hydro-meteorological conditions (in blue).

## 243 4 Results

### 244 4.1 Assess flash drought recovery time based on vegetation productivity

245 Given the prevalence of drought in regions over the past few decades, drought is a major natural disaster worldwide (WMO.  
246 2021). In addition, its exposure, vulnerability, and risk are expected to further increase under future climate and socio-  
247 economic changes (Tabari & Willems. 2018; Cook et al., 2020). Flash drought is widely recognized as a sub-seasonal  
248 phenomenon that develops rapidly (Tyagi et al., 2022). Flash droughts have varying degrees of impact on the photosynthesis,  
249 productivity, and respiration of ecosystems (Mohammadi et al., 2022). Reducing drought risks and strengthening social  
250 drought resistance are also important tasks in order to achieve SDGs by 2030 (Tabari et al., 2023). The response frequency  
251 of Solar-Induced Fluorescence (SIF) in the China basin to flash droughts exceeds 80%, with 96.85% of the regional response  
252 occurring within 16 days (Yang et al., 2023). Previous studies have calculated the recovery time of flash drought based on  
253 changes in soil moisture, ranging from 8 to 40 days (Otkin et al., 2019). Additionally, the recovery time is generally longer  
254 in humid areas compared to arid areas. However, not all flash drought events result in a decrease in ecosystem productivity  
255 (Liu et al., 2019). For instance, a study conducted by Zhang et al. (2020b) revealed that between 2003 and 2018, 81% of  
256 flash droughts in China displayed negative normalized anomalies in GPP, while the remaining 19% of the events did not  
257 exhibit such negative anomalies. Therefore, GPP serves as a more appropriate indicator for monitoring post-drought  
258 photosynthesis-related dynamics and evaluating ecosystem recovery time (Yu et al., 2017). Based on GPP, most flash



259 drought events in the Xiangjiang River Basin (XRB) and Weihe River Basin (WRB) recovered within 2 to 8 days. Moreover,  
260 the recovery time in the XRB, which is located in a humid area, tends to be longer (Wang et al., 2023). It should be noted  
261 that this study only investigated the aforementioned two watersheds and did not include semi-humid/semi-arid areas. Our  
262 study revealed that the average recovery time for flash droughts in the China is approximately 37.5 days (7.5 pentads)  
263 (Figure 3).

#### 264 4.2 The factors that affect drought recovery time

265 The solar radiation and aridity index were the primary factors that influence the recovery time (Figures 5 & 6). The recovery  
266 time was regulated by a combination of drought characteristics (drought return interval, severity, duration), post-drought  
267 hydro-meteorological conditions, and vegetation physiological characteristics (Fathi-Taperasht et al., 2022; Liu et al., 2019).  
268 In the case of flash droughts characterized by rapid development, the speed is one of the most important factors controlling  
269 the recovery time (Figure 6). Ecosystems experienced stress fatigue, which means that the restoration of the ecosystem  
270 progressively deteriorates due to repeated exposure to stressors that occur at frequencies outside the evolutionary history of  
271 the affected system (Hacke et al., 2001; Schwalm et al., 2017). Previous studies have shown that the spatial patterns of flash  
272 drought recovery were similar to those of precipitation, temperature, and radiation (Wang et al., 2023). Increased radiation  
273 energy and precipitation post a drought can promote vegetation photosynthesis (Zhang et al., 2021). Additionally, there are  
274 regional variations in the time required for drought recovery. Generally, semi-arid and semi-humid areas took longer to  
275 recover to their pre-drought state (Figure 5). Ecosystems in these areas exhibited higher overall sensitivity to drought  
276 (Vicente et al., 2013; Yang et al., 2016). Vegetation in arid areas adapted to long-term water deficit through various  
277 physiological, anatomical, and functional mechanisms, resulting in high drought resistance (Craine et al., 2013). In humid  
278 areas, sufficient water storage helped resist drought (Liu et al., 2018). Vegetation also played a crucial role in regulating the  
279 recovery trajectory. The drought resistance of plants was determined by various traits such as stomatal conductance,  
280 hydraulic conductivity, and cell turgor pressure (Bartlett et al., 2016; Martínez-Vilalta et al., 2017). Grasslands and  
281 shrublands could quickly recover from drought, while forest systems require longer periods of time (Gessler et al., 2017).  
282 This may be because those have relatively simple vegetation structures, shorter life cycles, and faster growth rates (Ru et al.,  
283 2023). In contrast, forest systems have more complex vegetation structures and ecological processes (Tuinenburg et al.,  
284 2022).

#### 285 4.3 Limitations and perspectives

286 We emphasized that the post-flash drought recovery trajectory of ecosystem is influenced by several factors, including post-  
287 flash drought hydrological conditions, flash drought characteristics, and the physiological characteristics of vegetation.  
288 However, we should note that in this study, the same percentile threshold (20%, 40%) was used to identify flash drought  
289 events based on empirical values from previous research findings. Further investigation should investigate how to determine  
290 region-specific thresholds and examine the sensitivity of these thresholds to flash drought recognition (Gou et al., 2022).



291 Furthermore, it is important to consider that plant strategies for coping with flash drought can vary due to species differences  
292 (Gupta et al., 2020). There is still a need for improvement in understanding the physiological and ecological mechanisms  
293 involved in flash drought recovery. Flash droughts can have multiple impacts on ecosystems, and it is worth noting that our  
294 approach in this study focused primarily on GPP. To gain a more comprehensive understanding, future research should  
295 explore the mechanism of ecosystem restoration from multiple perspectives, such as evaluating greenness and  
296 photosynthesis. In future water resource management, we should recognize the importance of adopting measures to reduce  
297 the risk of drought disasters.

## 298 **5 Conclusions**

299 Effectively reducing drought risk and reducing drought exposure are crucial for achieving sustainable development goals  
300 (SDGs) related to health and food security. This study applied a random forest regression model to analyze the factors  
301 influencing recovery time and the response functions settled up by partial correlation for typical flash drought recovery time.  
302 The most important environmental factor affecting recovery time is post-flash drought radiation, followed by aridity index  
303 and post-flash drought temperature. Recovery time prolongs with lower solar radiation conditions. Semi-arid/sub-humid  
304 areas have longer recovery time. Temperature does not exhibit a monotonic response in relation to recovery time;  
305 excessively cold or overheated temperatures lead to longer recovery times. Herbaceous vegetation recovers more rapidly  
306 than woody forests, with deciduous broadleaf forests demonstrating the shortest recovery time.

307 Our study assessed the recovery time of ecosystems to flash droughts based on GPP dataset and identified the dominant  
308 factors of recovery time. Results show that 78% of ecosystems could recover within 0 to 50 days. However, certain areas,  
309 such as central China and southern China, required 90 days or more to recover. The analysis of the response functions  
310 showed that radiation emerged as the most influential factor impacting flash drought recovery time, with lower solar  
311 radiation conditions leading to prolonged recovery time. Additionally, temperature did not exhibit a monotonic response in  
312 relation to recovery time. In terms of flash drought characteristics, the difference in recovery time is more associated with  
313 speed than severity and duration.

314 Although this study provides a good basis for further investigation of flash drought characteristics, it is important to note that  
315 the further extension of this study may lead to more understanding of flash drought for hydrological application or  
316 worldwide practices. It is important to determine region-specific thresholds and examine the sensitivity of these thresholds to  
317 flash drought recognition. Furthermore, plant strategies for coping with flash drought can vary due to species differences. To  
318 gain a more comprehensive understanding of flash drought recovery, future research should also explore the mechanism of  
319 ecosystem restoration from multiple perspectives, such as evaluating greenness and photosynthesis.

320



321 **Author contributions**

322 **Mengge Lu:** Conceptualization, Methodology, Data curation, Formal analysis, Writing - original draft. **Huaiwei Sun:**  
323 Conceptualization, Project administration, Writing - review & editing, Supervision. **Yong Yang:** Writing - review & editing.  
324 **Jie Xue:** Writing - review & editing. **Hongbo Lin:** Writing - review & editing. **HongZhang:** Writing - review & editing.  
325 **Wenxin Zhang:** Writing - review & editing.

326 **Declaration of competing interest**

327 The authors declare that they have no known competing financial interests or personal relationships that could have appeared  
328 to influence the work reported in this paper.

329 **Data availability**

330 Global Land Evaporation Amsterdam Model (GLEAM) soil moisture data is available from <https://www.gleam.eu/>. The  
331 China Meteorological Forcing Dataset (CMFD) can be accessed via [https://westdc.westgis.ac.cn/zh-hans/data/7a35329c-  
332 c53f-4267-aa07-e0037d913a21/](https://westdc.westgis.ac.cn/zh-hans/data/7a35329c-c53f-4267-aa07-e0037d913a21/). Global MODIS and FLUXNET-derived Product GPP dataset is available from  
333 <https://daac.ornl.gov>. The MODIS land cover dataset MCD12C1 is available from <https://doi.org/10.24381/cds.f17050d7>.

334 **Acknowledgements**

335 This study was funded by the Third Xinjiang Scientific Expedition Program (Grant No.2022xjkk0105) (H.S.). The authors  
336 also acknowledge funding from NSFC projects (51879110,52079055, 52011530128). In addition, H.S. acknowledges  
337 funding from a NSFC-STINT project (No. 202100-3211).

338 **References**

339 Bartlett, M. K., Klein, T., Jansen, S., Choat, B., & Sack, L., 2016. The correlations and sequence of plant stomatal,  
340 hydraulic, and wilting responses to drought. Proceedings of the National Academy of Sciences of the United States of  
341 America. 113(46), 13098-13103.

342 Chen, S. L., Xiong, L. H., Ma Q, et al., 2020. Improving daily spatial precipitation estimates by merging gauge observation  
343 with multiple satellite-based precipitation products based on the geographically weighted ridge regression method. Journal of  
344 Hydrology. 589: 125156.



- 345 Christian, J.I., Martin, E.R., Basara, J.B., et al., 2023. Global projections of flash drought show increased risk in a warming  
346 climate. *Commun Earth Environ.* 4, 165.
- 347 Craine, J. M., Ocheltree, T. W., Nippert, J. B., et al., 2013. Global diversity of drought tolerance and grassland climate-  
348 change resilience. *Nature Climate Change*, 3(1), 63–67.
- 349 Cook, B. I. et al., 2020. Twenty-first century drought projections in the CMIP6 forcing scenarios. *Earths Future* 8,  
350 e2019EF001461.
- 351 Darnhofer, I., Lamine, C., Strauss, A., et al., 2016. The resilience of family farms: Towards a relational approach. *Journal of*  
352 *Rural Studies*. 44: 111-122.
- 353 Fathi-Taperasht A, Shafizadeh-Moghadam H, Minaei M, et al., 2022. Influence of drought duration and severity on drought  
354 recovery period for different land cover types: evaluation using MODIS-based indices. *Ecological Indicators*. 141: 109146.
- 355 Friedl, M. A., McIver, D. K., Hodges, J. C. F., et al., 2002. Global land cover mapping from MODIS: Algorithms and early  
356 results. *Remote Sensing of Environment*. 83(1), 287-302.
- 357 Fu, Z., Li, D., Hararuk, O., et al., 2017. Recovery time and state change of terrestrial carbon cycle after disturbance.  
358 *Environmental Research Letters*. 12(10): 104004.
- 359 Gazol, A., Camarero, J. J., Anderegg, W. R. L., & Vicente-Serrano, S. M., 2017. Impacts of droughts on the growth  
360 resilience of northern hemisphere forests. *Global Ecology and Biogeography*. 26(2), 166–176.
- 361 Gazol, A., Camarero, J. J., Vicente-Serrano, S. M., et al., 2018. Forest resilience to drought varies across biomes. *Global*  
362 *Change Biology*. 24(5), 2143–2158.
- 363 Gessler, A., Schaub, M., McDowell, N. G., 2017. The role of nutrients in drought-induced tree mortality and recovery. *New*  
364 *Phytologist*. 214(2): 513-520.
- 365 Godde, C., Dizyee, K., Ash, A., et al., 2019. Climate change and variability impacts on grazing herds: Insights from a system  
366 dynamics approach for semi-arid Australian rangelands. *Global change biology*. 25(9): 3091-3109.
- 367 Gou, Q., Zhu, Y., Lü, H., et al., 2022. Application of an improved spatio-temporal identification method of flash droughts.  
368 *Journal of Hydrology*. 604: 127224.



- 369 Gupta, A., Rico-Medina, A., Caño-Delgado, A I., 2020. The physiology of plant responses to drought. *Science*. 368(6488):  
370 266-269.
- 371 Hacke, U. G., Stiller, V., Sperry, J. S., Pittermann, J. & McCulloh, K. A., 2001. Cavitation fatigue. Embolism and refilling  
372 cycles can weaken the cavitation resistance of xylem. *Plant Physiol.* 125, 779-786.
- 373 Hao, Y., Choi, M., 2023. Recovery of Ecosystem Carbon and Water Fluxes after Drought in China. *Journal of Hydrology*.  
374 129766.
- 375 He, B., Liu, J., Guo, L., et al., 2018. Recovery of ecosystem carbon and energy fluxes from the 2003 drought in Europe and  
376 the 2012 drought in the United States. *Geophysical Research Letters*. 45, 4879-4888.
- 377 Huang, J., Yu, H., Guan, X., Wang, G., & Guo, R., 2016. Accelerated dryland expansion under climate change. *Nature*  
378 *Climate Change*, 6(2), 16 6–171.
- 379 Jiao, T., Williams, C. A., De Kauwe, M. G., et al., 2021. Patterns of post-drought recovery are strongly influenced by  
380 drought duration, frequency, post-drought wetness, and bioclimatic setting. *Global Change Biology*, 27, 4630–4643.
- 381 Joiner, J., & Y. Yoshida. 2021. Global MODIS and FLUXNET-derived Daily Gross Primary Production, V2. ORNL DAAC,  
382 Oak Ridge, Tennessee, USA.
- 383 Kannenberg, S. A., Novick, K. A., Alexander, M. R., et al., 2019. Linking drought legacy effects across scales: From leaves  
384 to tree rings to ecosystems. *Global Change Biology*, 25(9), 2978–2992.
- 385 Kannenberg, S. A., Schwalm, C. R., & Anderegg, W. R. L., 2020. Ghosts of the past: How drought legacy effects shape  
386 forest functioning and carbon cycling. *Ecology Letters*. 23(5), 891–901.
- 387 Lenton, T. M., Held, H., Kriegler, E., et al., 2008. Tipping elements in the Earth's climate system. *Proceedings of the*  
388 *national Academy of Sciences*. 105(6), 1786-1793.
- 389 Lesinger, K., & Tian, D., 2022. Trends, variability, and drivers of flash droughts in the contiguous United States. *Water*  
390 *Resources Research*, 58, e2022WR032186.
- 391 Lindoso D P, Eiró F, Bursztyn M, et al., 2018. Harvesting water for living with drought: Insights from the Brazilian human  
392 coexistence with semi-aridity approach towards achieving the sustainable development goals. *Sustainability*, 10(3): 622.





- 393 Li, L., Yao, N., Li, Y., et al., 2019. Future projections of extreme temperature events in different sub-regions of China.  
394 Atmospheric research, 2019, 217: 150-164.
- 395 Liaw, A. & Wiener, M., 2002. Classification and regression by random forest. R News 2, 18-22.
- 396 Liu L, Gudmundsson L, Hauser M, et al., 2019. Revisiting assessments of ecosystem drought recovery. Environmental  
397 Research Letters. 14(11): 114028.
- 398 Liu, Y., van Dijk, A. I. J. M., Miralles, et al. 2018. Enhanced canopy growth precedes senescence in 2005 and 2010  
399 Amazonian droughts. Remote Sensing of Environment. 211, 26–37.
- 400 Liu, Y., Zhu, Y., Ren, L., et al., 2023. Flash drought fades away under the effect of accumulated water deficits: the  
401 persistence and transition to conventional drought. Environmental Research Letters. 18(11): 114035.
- 402 Lundberg, S. M., & Lee, S. I., 2017. A unified approach to interpreting model predictions. Advances in neural information  
403 processing systems, 30.
- 404 Martin, D. P., 2014. Partial dependence plots. <http://dpmartin42.github.io/posts/r/partial-dependence>.
- 405 Martínez-Vilalta, J., & Garcia-Forner, N., 2017. Water potential regulation, stomatal behaviour and hydraulic transport under  
406 drought: Deconstructing the iso/anisohydric concept. Plant, Cell and Environment. 40(6), 962–976.
- 407 Miyashita, K., Tanakamaru, S., Maitani, T., & Kimura, K., 2005. Recovery responses of photosynthesis, transpiration, and  
408 stomatal conductance in kidney bean following drought stress. Environmental and Experimental Botany. 53(2), 205–214.
- 409 Mohammadi, K., Jiang, Y., Wang, G., 2022. Flash drought early warning based on the trajectory of solar-induced  
410 chlorophyll fluorescence. Proceedings of the National Academy of Sciences. 119(32): e2202767119.
- 411 Nilsson, M., Griggs, D. & Visbeck, M., 2016. Policy: Map the interactions between Sustainable Development Goals. Nature  
412 534, 320–322.
- 413 Otkin, J. A., Zhong, Y., Hunt, E. D., et al., 2019. Assessing the evolution of soil moisture and vegetation conditions during a  
414 flash drought-flash recovery sequence over the South-Central United States. Journal of Hydrometeorology. 20(3): 549-562.
- 415 Peixoto, J. P. and Oort, A. H. 1996. The climatology of relative humidity in the atmosphere, Journal of Climate, 9, 3443-  
416 3463.



- 417 Poonia, V., Goyal, M. K., Jha, S., et al., 2022. Terrestrial ecosystem response to flash droughts over India. *Journal of*  
418 *Hydrology*. 605: 127402.
- 419 Qing, Y., Wang, S., Ancell, B.C., Yang, Z., 2022. Accelerating flash droughts induced by the joint influence of soil moisture  
420 depletion and atmospheric aridity. *Nat. Commun.* 13 (1).
- 421 Rigden, A. J., Mueller, N. D., Holbrook, N. M., Pillai, N., & Huybers, P. 2020. Combined influence of soil moisture and  
422 atmospheric evaporative demand is important for accurately predicting US maize yields. *Nature Food*, 1(2), 127–133.
- 423 Ru J, Wan S, Hui D, et al., 2023. Overcompensation of ecosystem productivity following sustained extreme drought in a  
424 semiarid grassland. *Ecology*. 104(4): e3997.
- 425 Schwalm, C., Anderegg, W., Michalak, A. et al., 2017. Global patterns of drought recovery. *Nature*. 548, 202-205.
- 426 Sreeparvathy, V., Srinivas, V.V., 2022. Meteorological flash droughts risk projections based on CMIP6 climate change  
427 scenarios. *npj Clim Atmos Sci* 5, 77.
- 428 Sun, H., Gui, D., Yan, B., et al., 2016. Assessing the potential of random forest method for estimating solar radiation using  
429 air pollution index. *Energy Conversion and Management*. 119, 121-129.
- 430 Tabari, H. & Willems, P., 2018. More prolonged droughts by the end of the century in the Middle East. *Environ. Res. Lett.*  
431 13, 104005.
- 432 Tabari, H., Willems, P. 2023. Sustainable development substantially reduces the risk of future drought impacts. *Commun*  
433 *Earth Environ* 4, 180.
- 434 Zotarelli, L., Dukes, M. D., Romero, C. C., et al., 2010. Step by step calculation of the Penman-Monteith Evapotranspiration  
435 (FAO-56 Method). Institute of Food and Agricultural Sciences. University of Florida, 8.
- 436 Štrumbelj, E., & Kononenko, I., 2014. Explaining prediction models and individual predictions with feature contributions.  
437 *Knowledge and information systems*, 41, 647-665.
- 438 Tuinenburg, O. A., Bosmans, J. H. C., Staal, A., 2022. The global potential of forest restoration for drought mitigation.  
439 *Environmental Research Letters*. 17(3): 034045.



- 440 Tyagi, S., Zhang, X., Saraswat, D., et al., 2022. Flash Drought: Review of Concept, Prediction and the Potential for Machine  
441 Learning, Deep Learning Methods. *Earth's Future*. 10(11): e2022EF002723.
- 442 Vicente-Serrano, S. M., Gouveia, C., Camarero, J. J., et al. 2013. Response of vegetation to drought time-scales across  
443 global land biomes. *Proceedings of the National Academy of Sciences of the United States of America*, 110(1), 52-57.
- 444 Wang, L., Yuan, X., Xie, Z., et al., 2016. Increasing flash droughts over China during the recent global warming hiatus. *Sci*  
445 *Rep.* 6:30571.
- 446 Wang, Y., & Yuan, X., 2022a. Land-atmosphere coupling speeds up flash drought onset. *Science of The Total Environment*,  
447 851, 158109.
- 448 Wang, S., Peng, H., & Liang, S., 2022b. Prediction of estuarine water quality using interpretable machine learning approach.  
449 *Journal of Hydrology*. 605, 127320.
- 450 Wang, H., Zhu, Q., Wang, Y., et al., 2023. Spatio-temporal characteristics and driving factors of flash drought recovery:  
451 From the perspective of soil moisture and GPP changes. *Weather and Climate Extremes*. 42: 100605.
- 452 WMO. 2021. WMO Atlas of Mortality and Economic Losses from Weather, Climate and Water Extremes (1970–2019).  
453 WMO-No. 1267.
- 454 Wu, X., Liu, H., Li, X., et al., 2017. Differentiating drought legacy effects on vegetation growth over the temperate Northern  
455 Hemisphere. *Global Change Biology*. 24(1), 504-516.
- 456 Xu, S., Wang, Y., Liu, Y., et al., 2023. Evaluating the cumulative and time-lag effects of vegetation response to drought in  
457 Central Asia under changing environments. *Journal of Hydrology*. 130455.
- 458 Yang, L., Wang, W., Wei, J., 2023. Assessing the response of vegetation photosynthesis to flash drought events based on a  
459 new identification framework. *Agricultural and Forest Meteorology*. 339: 109545.
- 460 Yang, K., He, J., Tang, W., et al., 2019. China meteorological forcing dataset (1979-2018). A Big Earth Data Platform for  
461 Three Poles. <https://doi.org/10.11888/AtmosphericPhysics.tpe.249369.file>.
- 462 Yang, L., Wang, W., Wei, J., 2023. Assessing the response of vegetation photosynthesis to flash drought events based on a  
463 new identification framework. *Agricultural and Forest Meteorology*. 339: 109545.



- 464 Yang, Y. T., Guan, H. D., Batelaan, O., et al., 2016. Contrasting responses of water use efficiency to drought across global  
465 terrestrial ecosystems. *Scientific Reports*, 6, 23284.
- 466 Yao, T., Liu, S., Hu, S., et al., 2022. Response of vegetation ecosystems to flash drought with solar-induced chlorophyll  
467 fluorescence over the Hai River Basin, China during 2001–2019. *Journal of Environmental Management*. 313: 114947.
- 468 Yu, Z., Wang, J., Liu, S., et al., 2017. Global gross primary productivity and water use efficiency changes under drought  
469 stress. *Environmental Research Letters*, 12(1), 014016.
- 470 Yuan, X., Wang, L., Wu, P., Ji, P., Sheffield, J., Zhang, M., 2019. Anthropogenic shift towards higher risk of flash drought  
471 over China. *Nat. Commun.* 10 (1).
- 472 Zha, X., Xiong, L., Liu, C., Shu, P., & Xiong, B., 2023. Identification and evaluation of soil moisture flash drought by a  
473 nonstationary framework considering climate and land cover changes. *Science of the Total Environment*, 856, 158953.
- 474 Zhang, X., Chen, N., Sheng, H., et al. 2019. Urban drought challenge to 2030 sustainable development goals. *Science of the*  
475 *Total Environment*. 693: 133536.
- 476 Zhang, M., Yuan, X., 2020a. Rapid reduction in ecosystem productivity caused by flash droughts based on decade-long  
477 FLUXNET observations. *Hydrology and Earth System Sciences*. 24(11): 5579-5593.
- 478 Zhang, M., Yuan, X., & Otkin, J. A., 2020b. Remote sensing of the impact of flash drought events on terrestrial carbon  
479 dynamics over China. *Carbon Balance and Management*, 15(1), 1-11.
- 480 Zhang, S., Yang, Y., Wu, X., et al., 2021. Post drought recovery time across global terrestrial ecosystems. *Journal of*  
481 *Geophysical Research: Biogeosciences*. 126(6): e2020JG005699.
- 482 Zhang, S., Li, M., Ma, Z., et al., 2023. The intensification of flash droughts across China from 1981 to 2021. *Clim Dyn.*  
483 <https://doi.org/10.1007/s00382-023-06980-8>.
- 484 Zomer, R.J., Xu, J. & Trabucco, A., 2022. Version 3 of the Global Aridity Index and Potential Evapotranspiration Database.  
485 *Sci Data* 9, 409.
- 486